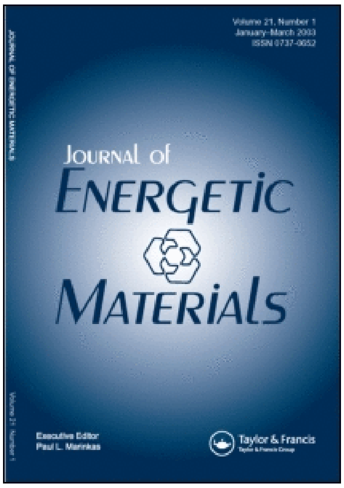

Journal of Energetic Materials
Publication details, including instructions for authors and subscription information:
http://www.informaworld.com/smpp/title~content=t713770432

Computational Study of Picric Acid and Potassium Picrate

Xue-Hai Ju[a]; Xiao-Juan Xu[a]; He-Ming Xiao[a]
[a] Department of Chemistry, Nanjing University of Science and Technology, Nanjing, People's Republic of China

To cite this Article Ju, Xue-Hai , Xu, Xiao-Juan and Xiao, He-Ming(2005) 'Computational Study of Picric Acid and Potassium Picrate', Journal of Energetic Materials, 23: 2, 121 — 130

To link to this Article: DOI: 10.1080/07370650590936442

URL: http://dx.doi.org/10.1080/07370650590936442

Energetic Materials, 23: 121–130, 2005

ISSN: 0737-0652 print
DOI: 10.1080/07370650590936442

Computational Study of Picric Acid and Potassium Picrate

XUE-HAI JU
XIAO-JUAN XU
HE-MING XIAO

Department of Chemistry, Nanjing University of
Science and Technology, Nanjing, People's
Republic of China

The density functional theory (DFT) method at the B3LYP/6-311+g** level was used for predicting the structures, natural bond orbital (NBO) atomic charges, thermodynamic properties, and IR spectroscopy of picric acid (PA) and potassium picrate (PP). The IR spectroscopies were assigned. The C–NO_2 bond is generally lengthier than all the other covalent bonds in both PA and PP, indicating that this bond is the weakest and prone to rupture in the decomposition process. The carbon atom that connects with oxygen atom in PP carries larger positive charges, and nitro oxygen atoms carry larger negative charges than the corresponding atoms in PA. The C–C populations of PP are more unevenly distributed than those of PA, indicating that the benzene ring of the former is less conjugated. Some C–C bonds in PP are much weaker. This weak C–C bond could be ruptured at the same time as the C–N bond in the initial decomposition process.

Keywords: molecular orbital calculations, picric acid, DFT, potassium picrate, properties

Address correspondence to Xue-Hai Ju, Department of Chemistry, Nanjing University of Science and Technology, Nanjing, 210094, People's Republic of China. E-mail: xhju@mail.njust.edu.cn

Introduction

Theoretical treatment of energetic molecules receives a wide range of recognition since it provides the necessary data needed for predicting the structures, thermodynamic properties, spectroscopy, bonding characteristics, and so on [1–6]. This information will be helpful for further investigation as well as molecular design of energetic compounds. Picric acid (PA) is an acidic nitro compound that reacts with metals and produces explosives of ignition such as potassium picrate (PP) [7,8]. So far as we know, there have been several theoretical investigations of these compounds. Chen *et al.* studied the molecular structures of picric acid by ab initio and density functional theory [9,10]. Zimpel *et al.* analyzed the geometric conformation and charge distribution in picric acid and alkali picrate salts using the SCF-MO method [11]. In this paper we performed full optimization on PA and PP by the DFT-B3LYP method [12,13]. On the basis of optimized structure and the IR spectra, thermodynamic properties were obtained. We also performed natural bond orbital (NBO) analyses to obtain reliable atomic charges.

Computational Methods

The title molecules obtained with Chem3D software were fully optimized at the DFT-B3LYP level by the Berny method [14,15] with a $6\text{-}311+G^{**}$ basis set. Natural bond orbital analyses and frequency calculations were performed on each optimized structure. The computed frequencies were used to derive the thermodynamic functions' heat capacity, enthalpy, and entropy employing the statistical thermodynamic method. All calculations were performed with the Gaussian98 program [16] at a Compaq Workstation in our laboratory. The default convergence cutoffs given in the program were used throughout the computations.

Results and Discussion

Optimized Geometries

The fully optimized structures for the title compounds are shown in Figure 1. Table 1 lists the optimized geometrical

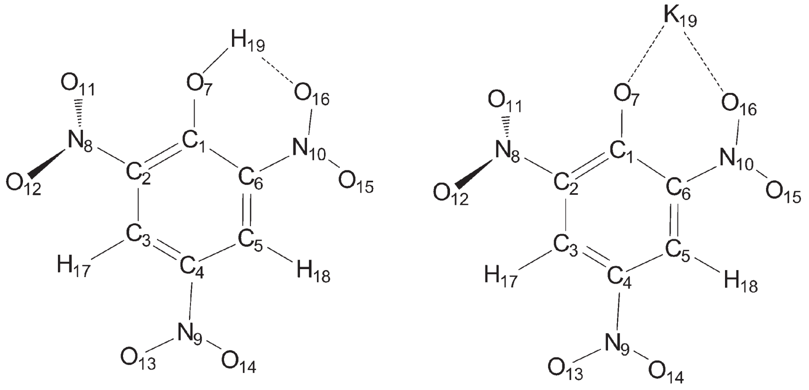

Figure 1. Molecular structures and atomic numbering of PA and PP.

parameters. The distances of both C1—C6 and C1—C2 are longer than all the other C—C bonds in the benzene ring due to the interaction of hydroxyl proton or potassium cation with the nitro group. As can be seen from Table 1, both lengths and angles of PP are in good agreement with experimental values [8,17] with the exception of the distance between atoms O and K. The potassium ion in the PP crystal contacts with two hydroxyl oxygen atoms, which makes the O—K length of the PP crystal to be ca. 0.03 pm lengthier than its isolated molecule. The O—K bond is ionic, since the K atom carries almost 1 a.u. positive charge, and at the same time the sum of negative charges on O7 and O16 is also about 1 a.u. (see Table 3 below). The C—NO_2 bond is generally lengthier than all the other covalent bonds in both PA and PP, indicating that this bond is the weakest and prone to rupture in the decomposition process.

NBO Charges, Mulliken Populations

Table 2 lists the NBO charges for both PA and PP. The NBO theory applies an interatomic orthogonalization step to establish asymmetrical atomic orbitals [18] and thus gives charges of relatively basis-set independence compared to other methods

Table 1

Optimized geometries of picric acid (PA) and potassium picrate (PP) at the B3LYP/6-311 + g** level^{a}

Parameters	PA	PP	Parameters	PA	PP
$R_{1\text{-}2}$	0.1414(0.1407)	0.1454(0.1452)	$\theta_{1\text{-}2\text{-}3}$	122.60(122.4)	124.30(124.57)
$R_{1\text{-}6}$	0.1422(0.1412)	0.1458(0.1452)	$\theta_{1\text{-}2\text{-}8}$	120.03	118.39
$R_{1\text{-}7}$	0.1317(0.1312)	0.1249(0.1245)	$\theta_{2\text{-}3\text{-}4}$	118.92	119.09
$R_{2\text{-}3}$	0.1378(0.1355)	0.137	$\theta_{3\text{-}4\text{-}5}$	121.55	121.05
$R_{2\text{-}8}$	0.1481(0.1477)	0.147	$\theta_{3\text{-}4\text{-}9}$	119.21(118.9)	119.43(118.98)
$R_{3\text{-}4}$	0.1393(0.1367)	0.1402	$\theta_{4\text{-}5\text{-}6}$	118.77(117.7)	119.75(118.55)
$R_{3\text{-}17}$	0.1082	0.1082	$\theta_{1\text{-}6\text{-}5}$	122.28	123.04
$R_{4\text{-}5}$	0.1381(0.1367)	0.1383(0.1385)	$\theta_{1\text{-}6\text{-}10}$	120.29(119.4)	120.66(119.41)
$R_{4\text{-}9}$	0.1477(0.1455)	0.1460(0.1444)	$\theta_{1\text{-}7\text{-}19}$	107.61	138.42
$R_{5\text{-}6}$	0.1390(0.1373)	0.1390(0.1373)	$\theta_{2\text{-}8\text{-}11}$	117.34	117.64
$R_{5\text{-}18}$	0.1081	0.1081	$\theta_{2\text{-}8\text{-}12}$	116.4	117.51

$R_{6\text{-}10}$	0.1465(0.1455)	0.1448(0.1463)	$\theta_{4\text{-}9\text{-}13}$	117.12	117.57
$R_{7\text{-}19}$	0.0986	0.2432(0.2740)	$\theta_{4\text{-}9\text{-}14}$	117.29(118.2)	117.88(118.49)
$R_{8\text{-}11}$	0.1218(0.1183)	0.1224	$\theta_{6\text{-}10\text{-}15}$	118.87(118.7)	118.99(117.62)
$R_{8\text{-}12}$	0.1223(0.1202)	0.1226	$\theta_{6\text{-}10\text{-}16}$	117.48(119.4)	118.96(119.38)
$R_{9\text{-}13}$	0.1222(0.1217)	0.1228	$\varphi_{2\text{-}1\text{-}7\text{-}19}$	178.42	−146.64
$R_{9\text{-}14}$	0.1222(0.1214)	0.1228	$\varphi_{1\text{-}2\text{-}8\text{-}11}$	43.77	41.64
$R_{10\text{-}15}$	0.1213(0.1201)	0.1223(0.1227)	$\varphi_{1\text{-}2\text{-}8\text{-}12}$	−138.08	−139.99
$R_{10\text{-}16}$	0.1244(0.1227)	0.1247(0.1223)	$\varphi_{5\text{-}4\text{-}9\text{-}13}$	−179.69	−179.35
$R_{16\text{-}19}$	0.1695(0.1680)	0.2567(0.2875)	$\varphi_{5\text{-}4\text{-}9\text{-}14}$	0.29(0.6)	0.71(5.5)
$\theta_{2\text{-}1\text{-}6}$	115.85(115.2)	112.55(111.63)	$\varphi_{1\text{-}6\text{-}10\text{-}15}$	−178.39	160.07
$\theta_{2\text{-}1\text{-}6}$	115.85(115.2)	112.55(111.63)	$\varphi_{1\text{-}6\text{-}10\text{-}15}$	−178.39	160.07
$\theta_{2\text{-}1\text{-}7}$	119.75(120.3)	122.39(124.19)	$\varphi_{1\text{-}6\text{-}10\text{-}16}$	1.68(7.4)	−21.22(−26.5)

[a] Bond length in nm, bond angle and dihedral angle in degrees; values in parentheses are from the experiments of [8] and [17] for PP and PA, respectively.

Table 2
NBO charges of PA and PP at the B3LYP/6-311 + G** level

Atoms	PA	PP	Atoms	PA	PP
C_1	0.3823	0.4303	O_{11}	−0.3287	−0.3705
C_2	0.0449	0.0101	O_{12}	−0.3581	−0.3803
C_3	−0.1295	−0.1380	O_{13}	−0.3610	−0.3904
C_4	0.0520	0.0190	O_{14}	−0.3653	−0.3924
C_5	−0.1353	−0.1337	O_{15}	−0.3267	−0.3672
C_6	0.0083	−0.0176	O_{16}	−0.4200	−0.5121
O_7	−0.6092	−0.7486	H_{17}	0.2798	0.2700
N_8	0.4887	0.4889	H_{18}	0.2855	0.2733
N_9	0.4888	0.4851	H_{19}/K_{19}	0.5082	0.9824
N_{10}	0.4956	0.4916			

such as Mulliken charges and their variations. As can be seen from Table 2, the C1, N, and H atoms of both PA and PP carry large positive charges, while all the oxygen atoms bear large negative charges. As the H19 is substituted by potassium, the positive charges on K19 are almost as large as twice those of H19, forming an ionic linkage of O7−K19 in PP instead of a covalent bond of O−H in PA. Another striking feature caused by substituting K for H is that the C1 atom in PP carries larger positive charges, and nitro oxygen atoms carry larger negative charges than the corresponding atoms in PA. The large positive

Table 3
Mulliken bonding populations of PA and PP

Bond	PA	PP
C−C	1.215–1.447	1.032–1.534
C−O	1.215	1.684
C−N	0.860–0.910	0.926–0.957
N−O	1.417–1.560	1.427–1.496
C−H	0.944–0.946	0.949–0.951

charges in the nitro oxygen atoms facilitate the formation of an ionic linkage between K19 and O16. This is also the reason that each potassium ion in the PP crystal contacts with two phenol oxygen atoms as well as with two nitro oxygen atoms.

Table 3 gives the Mulliken bonding populations of PA and PP. A striking feature of the Mulliken population is that the C−C populations of PP are more unevenly distributed than those of PA, indicating that the benzene ring of the former is less conjugated. The populations of C−N bonds for both PA and PP are smaller than those of all the other bonds, indicating that the C−N bond is prone to cleave upon impacting or other stimulats. In addition, some C−C bonds in PP are very weak, indicating that the weak C−C bond could be ruptured at the same time as the C−N bond in the initial decomposition process.

Vibrational Frequencies

The characterized vibrational frequencies (IR) with scaling factor of 0.96 and their intensities (KM/mol) were shown in Figure 2. As for PA, the mode of 3256 cm^{-1} associated with O−H stretching exhibits the largest IR intensity as the results of large dipole moment change. The C−H stretching mode is 3104 cm^{-1} along with a small intensity. The modes of 1549 and 1310 cm^{-1} belong to the stretching of N−O and C−N, respectively. All the other modes from 1260 to 1605 cm^{-1} associate with the stretching of the C−C and C−O bonds or with the deformation of the benzene skeleton. The mode of 1243 cm^{-1} associates with the rocking of C−H and O−H bonds, and 1049 cm^{-1} with the C−H rocking. As for PP, there is hardly any adsorption over 1630 cm^{-1}. The mode of 1595 cm^{-1} belongs to ring breathing and C−O stretching. The modes of 1544 and 1531 cm^{-1} belong to the stretching of C−C. The modes in a range of 1508–1297 cm^{-1} associate with the N−O, C−N, and C−C stretching and rocking. 1277 cm^{-1} belongs to the C−N stretching and C−H rocking. 1247 cm^{-1} is the ring deformation and C−C asymmetrical stretching. 1136 and 1048 cm^{-1} are the C−H rocking and scissor as well as the C−N symmetrical stretching.

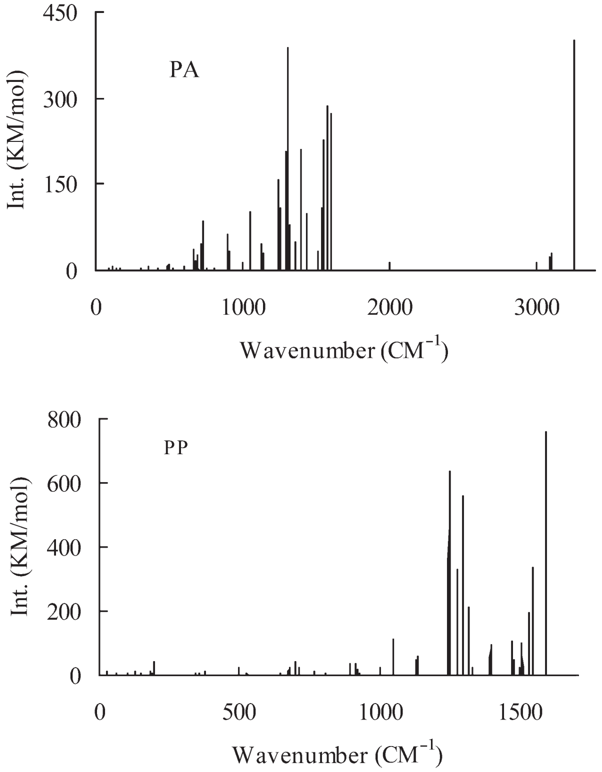

Figure 2. Vibrational frequencies and intensities.

Thermodynamic Properties

On the basis of vibrational analysis and statistical thermodynamic method, the standard thermodynamic functions, heat capacities ($C^0_{p,m}$), entropies ($S^0_{p,m}$), and enthalpies ($H^0_{p,m}$), were obtained and are listed in Table 4. As can be seen from the Table 4, the values of the three thermodynamic functions increase as temperature increases, due to the vibrational movement being intensified at high temperature and making a larger contribution to the thermodynamic functions. In addition, the increment of the ($C^0_{p,m}$) values becomes small as temperature increases, while the values of ($S^0_{p,m}$) and ($H^0_{p,m}$) increase constantly as temperature increases. On the basis of the ($C^0_{p,m}$)

Table 4

Thermodynamic properties at different temperatures[a]

	PA			PP		
T	$(C^0_{p,m})$	(S^0_m)	(H^0_m)	$(C^0_{p,m})$	(S^0_m)	(H^0_m)
298.15	211.13	494.89	37.63	230.13	544.31	42.75
400.00	258.59	563.80	61.63	275.67	618.53	68.59
500.00	295.72	625.65	89.43	311.11	684.01	98.00
600.00	324.47	682.22	120.50	338.39	743.25	130.54
700.00	346.67	733.98	154.10	359.27	797.05	165.47
800.00	363.99	781.45	189.67	375.41	846.13	202.23

[a] T/K, $(C^0_{p,m})/(\mathrm{J{\cdot}mol^{-1}{\cdot}K^{-1}})$, $(S^0_m)/(\mathrm{J{\cdot}mol^{-1}{\cdot}K^{-1}})$, $(H^0_m)/(\mathrm{kJ{\cdot}mol^{-1}})$. A scale factor of 0.96 is imposed for frequencies [19].

values, the following polynomial functions were obtained for the relationship between $(C^0_{p,m})$ and T at 298–700 K:

$$C^0_{p,m} = 34.236 + 0.7055T - 3.679 \times 10^{-4}T^2 \quad \text{for PA,}$$
$$C^0_{p,m} = 59.843 + 0.6807T - 3.589 \times 10^{-4}T^2 \quad \text{for PP.}$$

These equations, as well as the values of thermodynamic functions, provide valuable information for experimentalists.

Acknowledgment

X.H.J. thanks the Postdoctoral Foundation provided by the Education Ministry of the People's Republic of China for their support of this work.

References

[1] Xiao, H. M. 1993. *Molecular Orbital Theory for Nitro Compounds*, Beijing: National Defense Industrial Press.
[2] Zeman, S. 2002. *Thermochim. Acta*, 384: 137.
[3] Rice, B. M. and J. J. Hare. 2002. *J. Phys. Chem. A*, 106: 1770.
[4] Manaa, M. R., L. Fried, and E. J. Reed. 2003. *J. Comput. Aid Mol. Des.*, 10: 75.

[5] Ju, X. H., H. M. Xiao, and Q. Y. Xia. 2003. *J. Phys. Chem.*, 119: 10247.

[6] Xiao, H. M. and X. H. Ju. 2004. *Intermolecular Interactions in Energetic Systems*, Beijing: Science Press.

[7] Lao, Y. L. 1997. *Chemical Technology for Initiators.* Beijing: Beijing Institute of Technology Press.

[8] Shao, B., T. L. Zhang, J. G. Zhang, Y. M. Yang, L. Yang, and K. B. Yu. 2001. *Energetic Mater.*, 9: 122.

[9] Chen, P. C. and C. C. Huang. 1993. *J. Mol. Struct. (Theochem.)*, 282: 287.

[10] Chen, P. C. and S. C. Tzeng. 1999. *J. Mol. Struct. (Theochem.)*, 467: 243.

[11] Zimpel, Z., B. R. Nelson, and J. A. Weil. 1996. *Can J. Chem.*, 74: 70.

[12] Becke, A. D. 1993. *J. Chem. Phys.*, 98: 5648.

[13] Lee, C., W. Yang, and R. G. Parr. 1988. *Phys. Rev. B*, 37: 785.

[14] Fletcher, R. and M. J. D. Powell. 1963. *Comput. J.*, 6: 163.

[15] Schlegel, H. B. 1982. *J. Comput. Chem.*, 3: 214.

[16] Frisch, M. J., G. W. Trucks, H. B. Schlegel, et al. 1998. *Gaussian 98 (Revision A.7)*, Pittsburgh, PA: Gaussian, Inc.

[17] Duesler, E. N., J. H. Engelmann, D. Y. Curtin, et al. 1978. *Cryst. Struct. Comm.*, 7: 449.

[18] Reed, A. E., R. B. Weinstock, and F. Weinhold. 1985. *J. Chem. Phys.*, 83: 735.

[19] Pople, J. A., H. B. Schlegel, R. Krishnan, D. J. Defrees, J. S. Binkley, M. J. Frisch, R. A. Whiteside, R. F. Hout, and W. J. Hehre. 1981. *Int. J. Quantum Chem., Quantum Chem. Symp.*, 15: 269.